Available online at www.sciencedirect.com
SCIENCE DIRECT®
Biochimica et Biophysica Acta 1688 (2004) 10–17
BIOCHIMICA ET BIOPHYSICA ACTA
BBA
www.bba-direct.com

Role of lipid interactions in autoimmune demyelination

Benjamin Ohler[a,b], Karlheinz Graf[a], Richard Bragg[a], Travis Lemons[a], Robert Coe[a], Claude Genain[c], Jacob Israelachvili[b], Cynthia Husted[a,b,*]

[a] *Center for the Study of Neurodegenerative Disorders, Neuroscience Research Institute, Biological Sciences 2, University of California, Santa Barbara, CA 93106-5060, USA*
[b] *Department of Chemical Engineering, 3357 Engineering II, University of California, Santa Barbara, CA 93106, USA*
[c] *Department of Neurology, Room S-258, 505 Parnassus Avenue, University of California, San Francisco, CA 94143-0435, USA*

Received 9 June 2003; received in revised form 15 September 2003; accepted 17 October 2003

Abstract

A morphological transformation involving loss of adhesion between myelin lamellae and formation of myelin vesicles has been described as a mechanism for demyelination in multiple sclerosis and marmoset experimental allergic encephalomyelitis (EAE). Although protein interactions are involved in maintaining normal myelin structure, we describe here how lipids contribute to myelin stability and how lipid changes in EAE, including increases in lipid polyunsaturation and negatively charged phosphatidylserine (PS), promote demyelination. Three physico-chemical techniques were used to identify these changes: (1) Langmuir monolayer isotherms indicated that EAE white matter lipids were significantly more 'expanded' (fluid) than controls. (2) NMR spectroscopy indicated that EAE myelin lipids were more polyunsaturated than controls. (3) High-performance liquid chromatography (HPLC) with an evaporative light scattering detector indicated increased PS in EAE compared to controls, while sphingomyelin (SM), sulfatides and phosphatidylcholine (PC) were decreased. We present a physical model considering electrostatic, van der Waals and undulation forces to quantify the effect of these changes on myelin adhesion at the extracellular interface. Taken together, the isotherm, NMR, HPLC and modeling results support a mechanism for autoimmune demyelination whereby the composition of myelin lipids is altered in a manner that increases myelin fluidity, decreases myelin adhesion, increases membrane curvature, and promotes vesiculation.

Keywords: Experimental allergic encephalomyelitis; Myelin; Membrane lipid fluidity and packing; Multiple sclerosis

1. Introduction

Myelin is a stacked membrane structure (Figs. 1 and 2A) that allows for fast, efficient conduction of nerve impulses [1]. Multiple sclerosis (MS) is a neurodegenerative disorder characterized by the destruction of myelin (demyelination) with resultant loss of sensory and motor functions and disability [2]. The design of effective treatments for MS has been difficult, in part because the cause and exact mechanism of demyelination remain unknown.

While evidence that proteins play a structural role in myelin is significant [3], we have investigated the possibility that the myelin *lipids* contribute to myelin structure and adhesion. Indeed, the unusual abundance of lipids in myelin (~80% by dry mass) and their markedly asymmetric distribution across the myelin bilayers [1] suggest that they might play an important role and should not be ignored.

Toward investigating the role of lipids in myelin structure, prior work in our laboratory has focused on looking for very early alterations in the areas of MS brains that appeared normal macroscopically on in vivo standard spin echo magnetic resonance images and microscopically using in vitro standard histology. These studies found a variety of lipid composition changes that we believe reflect the early stages of a myelin lipid metabolism defect [4–6]. In the current study, we turned to the acute stage of active demyelination and examined myelin and white matter lipids isolated from acute experimental allergic encephalomyelitis (EAE) in the common marmoset (*Callithrix jacchus*) [7], a highly relevant model of MS. Recent ultrastructural studies of both marmoset EAE and selected cases of MS showed that myelin sheaths appear to disin-

* Corresponding author. Tel.: +1-805-893-4751; fax: +1-805-893-2005.
E-mail address: husted@lifesci.ucsb.edu (C. Husted).

0925-4439/$ - see front matter © 2003 Elsevier B.V. All rights reserved.
doi:10.1016/j.bbadis.2003.10.001

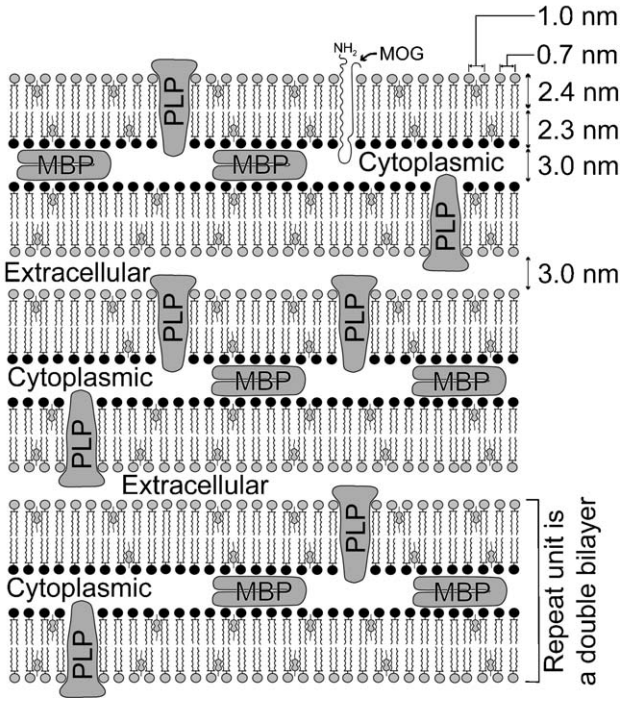

Fig. 1. Schematic diagram showing arrangement of lipids and proteins in myelin. Note the asymmetric distribution of lipids across the bilayer, where gray headgroups represent primarily sphingolipids (NCER, HCER, SCER, SM) and the black headgroups represent primarily phospholipids. Depicted protein shapes are schematic and used to show the protein distribution asymmetry and are not intended to imply that the true structure is completely known. Diagram constructed from literature values [1,37–39].

tegrate via a structural transformation that involves the loss of the normal compact, multilamellar structure (Fig. 2B) and formation of small vesicles (Fig. 2C) [8].

These structural changes drew our attention because they are very similar to the biophysical changes in membrane adhesion and curvature for which lipids have been proven to be responsible in other model and biological systems [9–11]. Membrane adhesion is determined by intermolecular interactions (i.e., van der Waals, electrostatic, undulation forces, etc.) that depend strongly on lipid properties (i.e., their charge and fluidity). Membrane curvature is also strongly correlated with the intrinsic molecular shapes of lipids (i.e., the relative areas of the headgroup vs. the acyl chains).

This paper describes the use of three complementary techniques to investigate the nature of brain lipid composition changes in marmoset EAE. The Langmuir monolayer technique was used because it is sensitive to lateral interactions between lipids, including their packing and fluidity [12]. Magic angle spinning (MAS) NMR spectroscopy was used as a measure of lipid acyl chain unsaturation and membrane fluidity. High-performance liquid chromatography (HPLC) was used for quantitative analysis of lipid class composition in the membranes. A simple physical model is presented that quantifies the effect of these changes and shows how they affect membrane curvature and intermembrane forces in a manner consistent with the observed ultrastructural transitions described by Genain et al. [8] (Fig. 2).

2. Materials and methods

2.1. Marmoset EAE and control white matter samples

Cerebral white matter samples were obtained immediately postmortem from 10 *C. jacchus* marmosets sensitized for acute EAE by active immunization with myelin antigens in adjuvant [8,13]. Routine histology confirmed varying degrees of inflammation accompanied by demyelination. Five identically processed samples were obtained from healthy marmosets (gift from Dr. Suzette Tardif, Kent State University). Lipids were extracted from dissected white matter using a modified Folch–Lees procedure [14,15]. Animals in this study were used in full compliance with all guidelines of the Institutional Animal Care and Use Committees.

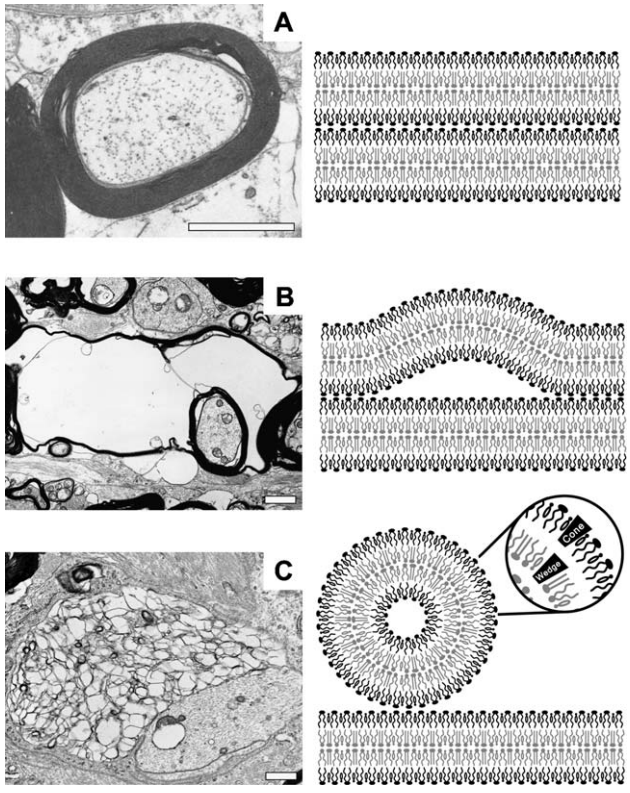

Fig. 2. Representative electron microscopy images (left column) along with schematic diagrams of myelin membrane morphological transitions (right column). Electron microscopy images are from the same data set published in Genain et al. [8] and were obtained as previously described. All scale bars indicate 1 μm. (A) Bilayers in normal myelin are stacked tightly, indicative of high intermembrane adhesion. (B) Myelin begins to lose adhesion and split along the extracellular lines. (C) The large myelin vacuoles appear to degrade into smaller vesicles with high membrane curvature, favored by "cone" lipids.

2.2. Lipids

The following nine purified brain-derived lipids with naturally occurring unsaturation were used as supplied commercially for model Langmuir isotherms and HPLC calibration: phosphatidylethanolamine (PE), phosphatidylcholine (PC), phosphatidylserine (PS), phosphatidylinositol, sphingomyelin (SM) (Avanti Polar Lipids, Alabaster, AL, 99%), cholesterol (CHOL), cholesterol esters (CE), α-hydroxy galactocerebrosides (HCER), non-hydroxy galactocerebrosides (NCER), (Sigma, St. Louis, MO, 99%), and cerebroside sulfates (sulfatides) (SCER) (Matreya, Pleasant Gap, PA, 98%).

2.3. Langmuir monolayers

Pressure–area (Π–A) isotherms of the lipids were measured at 22 °C (room temperature) on a Nima Technology 622 Langmuir trough (Coventry, England). Solutions of the lipids were made in a solvent of hexane/chloroform/ethanol (11:5:4, v/v) (Fisher Scientific, Pittsburgh, PA). The solutions were added dropwise onto the water surface and the solvent allowed to evaporate for 30 min. Isotherms were measured on compression at a speed of about 10 cm^2/min, which typically corresponded to about 1 $Å^2$/molecule/min.

2.4. HPLC analysis of lipids

The lipid composition of the white matter samples was determined by HPLC (Hewlett Packard 1100 series, Palo Alto, CA), with an Alltech Associates, Inc. Macrosphere GPC-100 7U diol column (Deerfield, IL) and an evaporative light scattering (mass) detector (Alltech Associates, model 500 ELSD) as described elsewhere [6,16,17].

2.5. MAS NMR analysis of white matter

Control and EAE marmoset white matter were analyzed with carbon-13 MAS NMR as described elsewhere [18]. Proton-decoupled carbon-13 MAS NMR Bloch decay spectra were acquired at 39 °C, marmoset body temperature, using an 11.7 T widebore superconducting NMR spectrometer (Chemagnetics, Fort Collins, CO).

2.6. Statistics

Standard two-tailed, unpaired t-tests were used to test for statistical significance in the comparison of EAE and control samples in Table 1 and Fig. 4.

2.7. Modeling of myelin interaction forces and adhesion

A simple model of myelin adhesion based on the so-called DLVO theory (van der Waals and electrostatic forces) [19,20] along with a repulsive thermal undulation force was used to gain insight into the biophysical significance of lipid changes in EAE. The interaction energy arising from the van der Waals force was modeled between two flat bilayers according to the equation:

$$E_{\mathrm{vdW}} = \frac{-A}{12\pi D^2} \ \{\mathrm{J\ m^{-2}}\} \tag{1}$$

where A is the Hamaker "constant" and D is the separation between the surfaces. Parsegian's formula for the Hamaker constant was used [21], given by:

$$A = A_{v=0}(1 + 2\kappa D)e^{-2\kappa D} + A_{v>v_1} \ \{\mathrm{J}\} \tag{2}$$

where $A_{v=0}$ is the unscreened zero-frequency contribution (taken as 0.3×10^{-20} J), κ is the reciprocal Debye length (1.25 nm^{-1} in physiological saline), and $A_{v>v_1}$ is the finite frequency contribution (taken as 0.5×10^{-20} J). This results in an unscreened Hamaker of 0.8×10^{-20} J at small separations that decays to 0.3×10^{-20} J beyond about one Debye length, as measured by Marra and Israelachvili [22] for typical lipid bilayers.

The electrostatic interaction [19,20] was modeled according to:

$$E_{\mathrm{DL}} = (\kappa^2/2\pi)Ze^{-\kappa D} \ \{\mathrm{J\ m^{-2}}\} \tag{3}$$

where κ is again the reciprocal Debye length and Z is a given by:

$$Z = 9.38 \cdot 10^{-11}\tanh^2(\psi_0/107) \ \{\mathrm{J\ m^{-1}}\} \tag{4}$$

for monovalent electrolytes at 37 °C and ψ_0 is the surface potential in units of millivolts [23]. The surface potential, in

Table 1
Lipid class composition of marmoset white matter for control and EAE samples by HPLC

Lipid Class	Controls (five samples)	EAE (five samples)[a]	Change vs. controls
Phosphatidylcholine (PC)$^{\pm}$	23.9 ± 0.4	18.1 ± 0.7	−24%[#]
Cholesterol (CHOL)	19.3 ± 2.2	22.6 ± 1.1	+17%
Cholesterol Esters (CE)	0.5 ± 0.1	1.5 ± 0.4	+200%[#]
Phosphatidylethanolamine (PE)$^{\pm}$	17.8 ± 0.5	19.7 ± 1.0	+11%
Hydroxy cerebrosides (HCER)	17.4 ± 1.8	18.8 ± 0.9	+8%
Cerebroside sulfates (SCER)$^{-}$	9.0 ± 0.1	5.4 ± 0.5	−40%[#]
Sphingomyelin (SM)$^{\pm}$	5.4 ± 0.1	1.8 ± 0.2	−67%[#]
Phosphatidylserine (PS)$^{-}$	3.8 ± 0.4	8.9 ± 0.5	+134%[#]
Non-hydroxy cerebrosides (NCER)	2.9 ± 0.5	3.1 ± 0.3	+7%[#]

Quantities are mass percent of dry weight, plus or minus standard error.
[a] Five of the ten EAE samples were analyzed earlier with NMR before the HPLC or monolayer analysis was available.
[#] Indicates $P < 0.05$ using a two-tailed, unpaired t-test.

turn, can be calculated from the Graham equation for a given charge density, σ, by:

$$\psi_0 = 53.4\sinh^{-1}(8.62\sigma[\mathrm{NaCl}]^{-1/2}) \ \{\mathrm{mV}\} \quad (5)$$

for 1:1 electrolytes at 37 °C [23], where [NaCl] is in units of mol l^{-1} and the charge density, in units of C m^{-2}, was calculated from the lipid composition and an assumed molecular area of 50 $Å^2$. The separation distance, D, was made uniformly 0.4 nm less than the separation for the van der Waals or undulation forces to account for the outer Helmholtz plane being farther out than the plane of origin of these forces (cf. Ref. [22]).

Thermal undulations result in a repulsive contribution to the potential energy of:

$$E_{\mathrm{und}} = \frac{3\pi^2(kT)^2}{128k_cD^2} \ \{\mathrm{J\ m^{-2}}\} \quad (6)$$

where k_c is the bending modulus of the lipid bilayer [10,24]. The above three terms were simply added together to get the overall potential energy curve for the myelin adhesion interaction. The energy units were converted from J m^{-2} to kT per molecule, again assuming an area of 50 $Å^2$ per molecule.

3. Results

3.1. HPLC results

Table 1 gives the lipid class compositions of marmoset control and EAE white matter samples as determined by HPLC. Significant decreases were found in SCER, PC and SM. Significant increases were found in NCER, PS, and CE with a trend for increases in CHOL. Phosphatidylinositol occurred below the quantifiable detection limit in all brain lipid samples.

3.2. Langmuir monolayer results

Fig. 3A shows isotherms of marmoset control and EAE white matter lipids. EAE isotherms (dashed) are shifted to significantly higher molecular areas and have smaller, less prominent kinks and plateaus around $\Pi_0 = 30–40$ mN/m compared to the controls.

Fig. 3B shows isotherms measured for two lipid solutions made from purified myelin lipid classes with compositions matching the average control and EAE compositions given in Table 1. These isotherms were measured to test the possibility that changes in lipid headgroup class alone (rather than acyl chains) drive the observed changes in the EAE isotherms. It is readily apparent that these isotherms do not exhibit the differences seen in Fig. 3A, which suggests that the observed isotherm changes for EAE samples are due to alterations in acyl chain composition (increased chain unsaturation), not lipid headgroup class composition. A series of isotherms demonstrating the effect of acyl chain composition is shown in Fig. 3C, where isotherms of various PC species show a pronounced expansion of the monolayers to larger molecular areas with increasing acyl chain unsaturation. Taken together, the data in Fig. 3 indicates that the EAE lipids have increased average surface areas relative to controls, and that this expansion is caused by an increase in acyl chain unsaturation, not by changes in lipid class (headgroup) concentration.

The isotherm results serve as a bulk measurement of the total lipid unsaturation, not as an overall thermodynamic model of the myelin membrane. Using Langmuir monolayers as a model of myelin assembly would have to account for the lipid asymmetry of the membrane, the effect of membrane proteins, the temperature and the ionic environment. For these reasons, attempts to experimentally model myelin assembly are probably better left to studies of bulk lipid solutions [25] and supported bilayers [26].

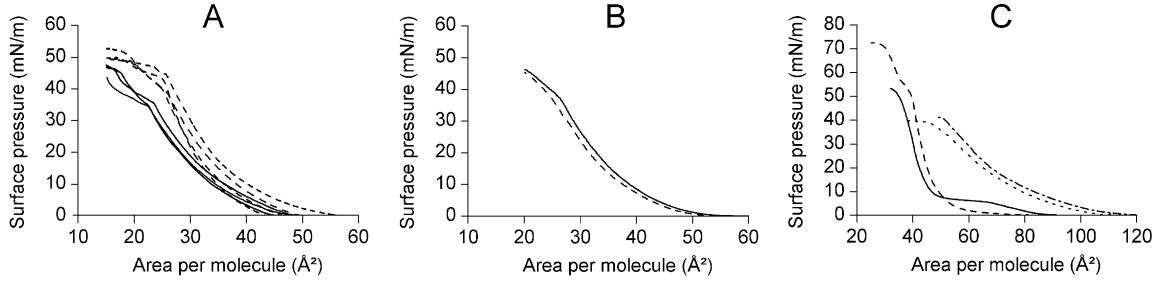

Fig. 3. Pressure–area (Π–A) isotherms of tissue extracted white matter lipids measured at 22 °C on pure water. (A) Marmoset EAE samples (dashed lines) show larger average molecular areas than controls (solid lines). Each isotherm represents a different tissue sample from a different individual marmoset. (B) Isotherms of model mixtures made from individual lipids having the same average composition of marmoset control (solid lines) and EAE (dashed lines) white matter are not significantly different. (C) Isotherms of pure synthetic PC species with increasing acyl chain unsaturation show a trend for more fluid, expanded monolayers. From left to right, acyl chain composition is 16:0–16:0 (solid), 16:0–18:0 (dashed), 16:0–18:2 (dotted), and 16:0–20:4 (dash-dot).

3.3. NMR results

An overall measure of myelin acyl chain composition and changes in EAE was obtained with MAS NMR spectroscopy [18]. MAS NMR is advantageous because no sample derivatization is required for lipid analysis and it is sensitive to both membrane lipid composition and molecular dynamics—a direct measure of membrane fluidity. For MAS NMR studies, the sample is not dissolved in solvent and the myelin membrane remains in its native multilamellar state. Fig. 4A shows the carbon-13 MAS NMR peaks corresponding to the double bonds of unsaturated acyl chains of myelin lipids. Each of the two peaks in Fig. 4A represents a superposition of several fatty acid resonances [18], but in general, the peak labeled "mono" represents primarily monounsaturated fatty acids (mainly 18:1, 24:1) and the peak labeled "poly" represents polyunsaturated fatty acids such as 18:2, 20:4 and 22:6. The increasing poly- to monounsaturated acyl chain ratio in Fig. 4 indicates that the acyl chains of EAE lipids are significantly more polyunsaturated than controls, a result consistent with the expanded pressure–area isotherms of Fig. 3A.

Because MAS NMR response is sensitive to both composition and fluidity while HPLC is sensitive only to composition, a comparison of NMR and HPLC results can provide semi-quantitative evidence of changing membrane fluidity. For example, a comparison of NMR and HPLC results for EAE and control white matter is shown in Fig. 4B. By HPLC, there is a 33% decrease in the concentration of PC and SM, but by MAS NMR, there appears to be a 34% *increase*. The increase in the NMR signal despite the decrease in concentration is explained by enhanced NMR relaxation dynamics in the EAE samples relative to controls. Because the NMR signal is proportional to concentration multiplied by a relaxation (fluidity) factor, the NMR results can be divided by the HPLC-measured composition results to isolate changes in the fluidity factor (Fig. 4C). Depending on the region of the correlation curve in which the measurement is made, this change in the "fluidity factor" could indicate either an increase or decrease in membrane fluidity. However, only increased fluidity is consistent with both the expanded EAE lipid isotherms (Fig. 3A) and the poly- to mono-NMR data (Fig. 4A). The fluidity factor of EAE samples is about twice that of controls, reflecting significantly greater fluidity. This is consistent with the observation of expanded vacuoles of myelin in acute EAE (Fig. 2B).

3.4. Effects on bilayer interaction energy

The model of myelin adhesion described above was used to investigate the effect of the observed lipid changes at the extracellular interface of myelin. The three key parameters that determine this adhesion are the charge or electrostatic potential of the membrane surface, the Hamaker constant, and the bending modulus of the membrane. The surface potential can be estimated relatively easily and accurately from the lipid composition data (for PS and SCER, the two charged lipids) and an average molecular area. Using Eq. (5), these calculations yielded surface potentials of $\psi_0 = -44$ mV for controls and -58 mV for EAE. The Hamaker constant for lipid bilayers has been found to be rather insensitive to the exact lipid species, so the assumed values of $A = 0.8 \times 10^{-20}$ J at small separations and 0.3×10^{-20} J at large separations

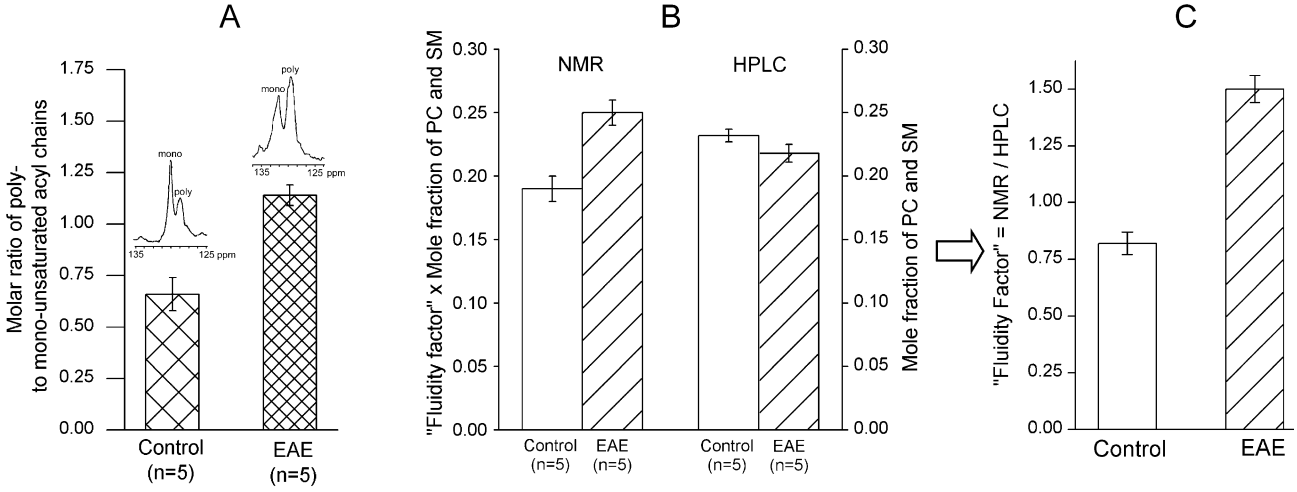

Fig. 4. (A) Comparison of acyl chain composition as measured by NMR. The increase in the poly- to mono- ratio indicates that the EAE lipids are significantly more polyunsaturated than the control lipids. Bars indicate standard errors. The difference was found to be statistically significant with $P < 0.05$. (B) Comparison of HPLC composition results to NMR response results. PC and SM are grouped together because NMR detects the headgroups, which are the same for these two lipids. The differences between control and EAE groups were statistically significant ($P < 0.05$) for both NMR and HPLC groups. Additionally, HPLC control results were significantly different from NMR control results, and HPLC EAE results were significantly different from NMR EAE results ($P < 0.05$). (C) Because NMR response is proportional to both composition and relaxation dynamics (which reflect membrane fluidity), a comparison of NMR response to HPLC absolute concentration data yields information on changes in fluidity. This "fluidity factor" has been isolated here by dividing the NMR response by the absolute concentration measured by HPLC. We find that this "fluidity factor" nearly doubles.

should be reliable estimates [27]. The major unknown in these calculations is the bilayer bending modulus, k_c. Experimental reports of the bending modulus for lipid membranes have focused on vesicles formed from a single lipid species or binary mixtures of lipids (usually a phospholipid and cholesterol) rather than natural mixtures. One study that examined the effect of chain unsaturation on the bending modulus of PC bilayers found that the number of double bonds in the chains was more important than their position or the chain length in determining the bending modulus. This group reported that measurements on bilayers of saturated and monounsaturated lipids yielded bending moduli of about 0.9×10^{-19} J, while bilayers of polyunsaturated lipids measured about 0.4×10^{-19} J [28]. However, a more recent report with a technique that better isolates only the bending of the membrane yielded a much smaller value of 0.46×10^{-19} J for bilayers of the *saturated* lipid DMPC in water at 30 °C [29]. This same paper reports that DMPC bilayers appear more flexible in buffer rather than in pure water ($k_c = 0.27 \times 10^{-19}$ J at 30 °C, and 0.15×10^{-19} J at 40 °C). Note that both temperatures are already above the phase transition temperature of 24 °C for DMPC [30]. Since there is no clear consensus as to the true magnitude of k_c, we have conservatively estimated a value of 0.6×10^{-19} J for control lipids (a value in the middle of the range) and 0.3×10^{-19} J for EAE lipids (assuming an effect of polyunsaturation similar to that reported by Rawicz et al. [28]). Using these values and the equations above, the plots in Fig. 5 are obtained. Fig. 5A shows the three contributions to the overall normal adhesive interaction potential energy for controls. Fig. 5B shows the overall energy plots for the control and EAE values, which indicate that the intermembrane interaction becomes completely repulsive at all separations. The shaded regions around each line in Fig. 5B indicate the variation of the adhesion energy for values of k_c in the range ± 25% from the values given above. Calculations (not shown) considering the increased electrostatic and undulation forces individually indicated that the increased undulation force (due to increased polyunsaturation) dominates the overall effect, reducing the interaction energy by 98%. The increased electrostatic force (due to increased PS) has a relatively minor effect, reducing the interaction energy by only 5%. Myelin lipid unsaturation therefore appears to be a key determinant of myelin stability.

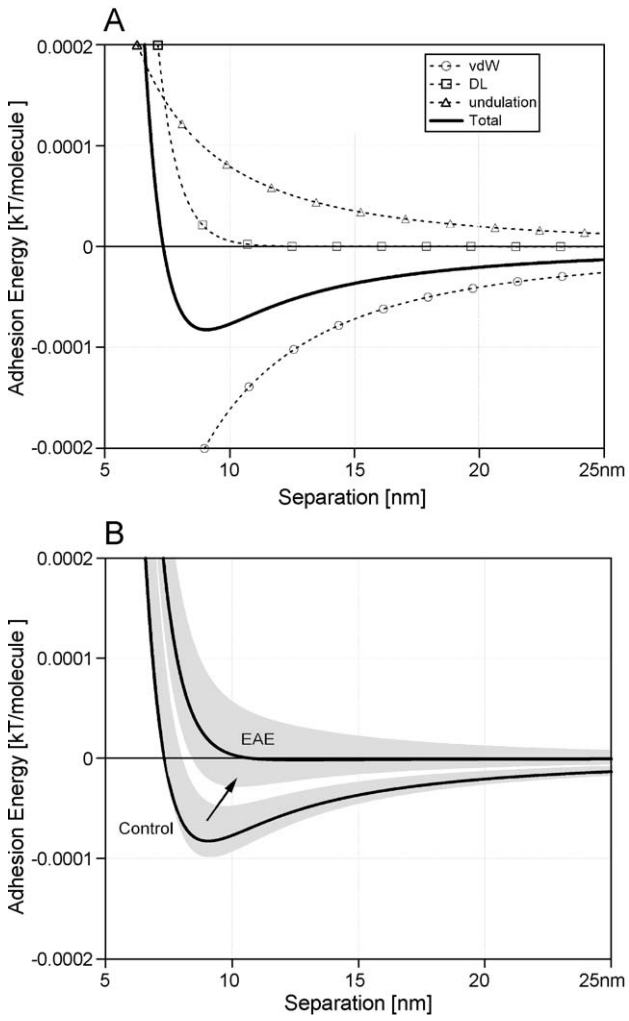

Fig. 5. (A) Total interaction energy plot (solid line) calculated using the control lipid composition indicates an adhesive energy minimum at 9 nm. The individual contributions to the total are shown with dashed lines, as labeled. Parameters used were $A = 0.8 \times 10^{-20}$ J at small separations, $A = 0.3 \times 10^{-20}$ J at large separations, $\psi_0 = -44$ mV and $k_c = 0.6 \times 10^{-19}$ J. (B) Calculations using the EAE lipid composition resulted in interaction energies that are repulsive at all separations, indicating that the myelin would swell. Parameters used for the EAE plot were $A = 0.8 \times 10^{-20}$ J at small separations, $A = 0.3 \times 10^{-20}$ J at large separations, $\psi_0 = -58$ mV and $k_c = 0.3 \times 10^{-19}$ J. The shaded regions surrounding each line represent the variation in the total energy if k_c is varied ± 25% from the assumed values (0.45×10^{-19} to 0.75×10^{-19} J for controls and 0.23×10^{-19} to 0.38×10^{-19} J for EAE), holding the other parameters constant.

3.5. Effects on bilayer curvature

Adhesion between adjacent bilayers can also be altered by changes in the spontaneous curvature of the membranes. The intrinsic molecular shape of the lipids, in particular, the area of the headgroup relative to the acyl chains influences membrane curvature. This observation is quantified using the "shape factor," $s = v/a_0 l_c$, where v is the hydrocarbon volume of the lipid, a_0 is the optimal headgroup surface area, and l_c is the critical length beyond which the chains are energetically constrained from exceeding [10]. This theory predicts increasingly convex curvature (e.g., curved bilayers → cylindrical micelles → spherical micelles) for values of $s < 1$, planar bilayers for $s \approx 1$, and increasingly convex curvature (e.g., inverted micelles) for $s > 1$. Note that the quantity v/l_c is approximately constant for diacyl lipids regardless of chain length or unsaturation because $v \propto l_c$. Therefore, changes in the headgroup area, a_0, tend to drive curvature changes. As the packing area of the EAE lipids appears to be changing relative to the controls (see Fig. 3A), this effect could certainly contribute to loss of adhesion and formation of vesicles depicted in Fig. 2.

4. Discussion

4.1. The role of lipids in determining myelin stability

It has been noted that the stable structure of normal myelin is the result of a delicate balance of forces to maintain its compact structure [31]. This is based on the observation that many processes, including both natural diseases and animal models, lead to demyelination despite the fact that their mechanistic details (what lipids or proteins are altered) vary widely. This suggests that a disturbance in any one or more myelin components could disrupt normal myelin structure [31]. One important implication of this observation is that although myelin proteins may contribute a portion of myelin intermembrane adhesion, myelin lipids also contribute to the adhesion and may be critical for maintaining the balance of forces and membrane stability. Despite many studies directed at finding a myelin protein defect in MS, none has conclusively been shown [32], with the possible exception of a myelin basic protein (MBP) alteration in rare cases of acute, fulminating (Marburg variant) MS [33]. Thus we have investigated the role of lipids and found dramatic changes in EAE myelin lipids relative to controls, the biophysical significance of which are discussed below.

4.2. The forces maintaining normal myelin structure

Normal, compact myelin forms a stacked bilayer structure like that shown schematically and by electron microscopy in Figs. 1 and 2A. In this form, adhesion between bilayers is strong and membrane curvature is low. We propose that different mechanisms maintain this adhesion at the cytoplasmic surfaces (major dense line) and the extracellular surfaces (intraperiod line). At the cytoplasmic interface, MBP most likely contributes the majority of the adhesion via attractive electrostatic interactions (ionic bonds or salt bridges) between its positively charged surface groups (mainly arginines) and the negatively charged PS present at that interface. Combined with the attractive van der Waals force, this easily offsets a repulsive force due to thermal undulations and accounts for the observation that the major dense line is exceptionally stable even when attempts are made to disrupt it ex vivo [34].

The situation at the extracellular interface is very different. Here, the only protein in any large quantity is proteolipid protein (PLP) which, although proposed to play an adhesive role [35], probably only interacts via weak van der Waals forces with the apposing membrane. The sulfatides present at this interface will contribute a repulsive force along with the repulsive force originating from thermal undulations. Evidently, the sum of these repulsive forces is offset by the attractive van der Waals interaction in normal myelin. Hence, we propose that adhesion at this interface is much less stable than at the cytoplasmic interface, an observation consistent with reports that loss of adhesion normally occurs at this interface in demyelinating diseases [8,36].

4.3. Lipid changes in EAE eliminate adhesion

In MS and EAE, demyelination appears to involve loss of the compact multilamellar structure (Fig. 2B) and subsequent degradation into small vesicles (Fig. 2C). The splitting occurs at the extracellular interface (intraperiod line) which implies a loss of intermembrane adhesion at this interface. For this to occur, the attractive van der Waals forces described above must be overcome by stronger repulsive forces arising from an increase in the thermal undulation and electrostatic forces. The physical model presented in Fig. 5A confirms that the intermembrane interaction should be adhesive for the control lipid composition. The model predicts that this adhesion is eliminated, becoming repulsive at all separations for the EAE composition (Fig. 5B). It should be noted, however, that even if the interaction energy minimum were only to be decreased, not eliminated (c.f. the shaded regions in Fig 5B), an alternative bilayer arrangement (i.e., vesicles) could then be more energetically favorable and therefore drive the equilibrium away from normal myelin structure. Clearly the bending modulus of the membrane is critically important, and a better understanding of exactly how polyunsaturation, buffer composition and temperature affect this parameter would be of great value.

In summary, our study suggests that myelin lipids contribute to acute immune-mediated demyelination by decreasing intermembrane adhesion, mainly due to an increase in polyunsaturation and negatively charged PS compared to controls. Understanding the origin of these lipid changes could provide a means to discover suitable methods for preventing myelin damage, for example, via an administration to restabilize myelin by counteracting the effects of increased fluidity and decreased adhesion or modifying the in vivo lipid synthesis processes.

Acknowledgements

The authors thank Centaur Pharmaceuticals Inc. (Sunnyvale, CA), the University of California Biotechnology Program, and the National Multiple Sclerosis Society (RG2795-A-3 to CH and JF2087-A-2 to CG). We thank Dr. Cedric Raine at Albert Einstein College of Medicine for the electron micrographs shown here. We also thank Dr. Suzette Tardif of Kent State University for her contribution of the control marmoset brains. Shadi Jahangir and Wendy See provided valuable technical assistance. Joe Zasadzinski, Yufang Hu and Richard Eckman provided valuable discussions and comments. Jan Post assisted with initial MAS NMR experiments of EAE white matter.

References

[1] P. Morell, Myelin, Plenum, New York, 1984.
[2] A. Compston, G. Ebers, H. Lassmann, McAlpine's Multiple Sclerosis, Churchill Livingstone, London, 1998.
[3] K.A. Williams, C.M. Deber, The structure and function of central nervous system myelin, Crit. Rev. Clin. Lab. Sci. 30 (1993) 29–64.
[4] C.A. Husted, D.S. Goodin, J.W. Hugg, A.A. Maudsley, J.S. Tsuruda, S.H. de Bie, G. Fein, G.B. Matson, M.W. Weiner, Biochemical alterations in multiple sclerosis lesions and normal-appearing white matter detected by in vivo ^{31}P and ^{1}H spectroscopic imaging, Ann. Neurol. 36 (1994) 157–165.
[5] C.A. Husted, G.B. Matson, D.A. Adams, D.S. Goodin, M.W. Weiner, In vivo detection of myelin phospholipids in multiple sclerosis with phosphorus magnetic resonance spectroscopic imaging, Ann. Neurol. 36 (1994) 239–241.
[6] B. Ohler, I. Revenko, C. Husted, Atomic force microscopy of non-hydroxy galactocerebroside nanotubes and their self-assembly at the air–water interface, with applications to myelin, J. Struct. Biol. 133 (2001) 1–9.
[7] C.P. Genain, S.L. Hauser, Experimental allergic encephalomyelitis in the new world monkey *Callithrix jacchus*, Immunol. Rev. 183 (2001) 159–172.
[8] C.P. Genain, B. Cannella, S.L. Hauser, C.S. Raine, Identification of autoantibodies associated with myelin damage in multiple sclerosis, Nat. Med. 5 (1999) 170–175.
[9] J.N. Israelachvili, Refinement of the fluid–mosaic model of membrane structure, Biochim. Biophys. Acta 469 (1977) 221–225.
[10] J. Israelachvili, Intermolecular and Surface Forces, Academic Press, San Diego, 1992.
[11] A. Schmidt, M. Wolde, C. Thiele, W. Fest, H. Kratzin, A.V. Podtelejnikov, W. Witke, W.B. Huttner, H.D. Soling, Endophilin I mediates synaptic vesicle formation by transfer of arachidonate to lysophosphatidic acid, Nature 401 (1999) 133–141.
[12] M.N. Jones, D. Chapman, Micelles, Monolayers, and Biomembranes, Wiley-Liss, New York, 1995.
[13] C.P. Genain, S.L. Hauser, Creation of a model for multiple sclerosis in *Callithrix jacchus* marmosets, J. Mol. Med. 75 (1997) 187–197.
[14] W.W. Christie, Lipid analysis: Isolation, Separation, Identification, and Structural Analysis of Lipids, Pergamon, Oxford, 1982.
[15] J. Folch, M. Lees, G.H.S. Stanley, A simple method for the isolation and purification of total lipides from animal tissues, J. Biol. Chem. 226 (1957) 497–509.
[16] W.W. Christie, Rapid separation and quantification of lipid classes by high performance liquid chromatography and mass (light-scattering) detection, J. Lipid Res. 26 (1985) 507–512.
[17] W.W. Christie, Separation of lipid classes by high-performance liquid chromatography with the "mass detector", J. Chromatogr. 361 (1986) 396–399.
[18] C. Husted, B. Montez, C. Le, M.A. Moscarello, E. Oldfield, Carbon-13 "magic-angle" sample-spinning nuclear magnetic resonance studies of human myelin, and model membrane systems, Magn. Reson. Med. 29 (1993) 168–178.
[19] E.J.W. Verwey, J.T.G. Overbeek, Theory of the Stability of Lyophobic Colloids, Elsevier, Amsterdam, 1948.
[20] B.V. Derjaguin, L. Landau, Theory of the stability of strongly charged lyophobic sols and of the adhesion of strongly charged particles in solutions of electrolytes, Acta Physicochim. URSS 14 (1941) 633–662.
[21] V.A. Parsegian, in: H. Van Olphen, K.J. Mysels (Eds.), Physical chemistry: Enriching topics from colloid and surface science, International Union of Pure and Applied Chemistry. Commission I.6: Colloid and Surface Chemistry, Theorex, La Jolla, CA, 1975, pp. 27–72.
[22] J. Marra, J. Israelachvili, Direct measurements of forces between phosphatidylcholine and phosphatidylethanolamine bilayers in aqueous electrolyte solutions, Biochemistry 24 (1985) 4608–4618.
[23] D. Leckband, J. Israelachvili, Intermolecular forces in biology, Q. Rev. Biophys. 34 (2001) 105–267.
[24] W. Helfrich, Steric interaction of fluid membranes in multilayer systems, Z. Naturforsch. A 33A (1978) 305–315.
[25] P. Riccio, A. Fasano, N. Borenshtein, T. Bleve-Zacheo, D.A. Kirschner, Multilamellar packing of myelin modeled by lipid-bound MBP, J. Neurosci. Res. 59 (2000) 513–521.
[26] H. Haas, M. Torrielli, R. Steitz, P. Cavatorta, R. Sorbi, A. Fasano, P. Riccio, A. Gliozzi, Myelin model membranes on solid substrates, Thin Solid Films 329 (1998) 627–631.
[27] J.N. Israelachvili, Strength of van der Waals attraction between lipid bilayers, Langmuir 10 (1994) 3369–3370.
[28] W. Rawicz, K.C. Olbrich, T. McIntosh, D. Needham, E. Evans, Effect of chain length and unsaturation on elasticity of lipid bilayers, Biophys. J. 79 (2000) 328–339.
[29] G. Althoff, O. Stauch, M. Vilfan, D. Frezzato, G.J. Moro, P. Hauser, R. Schubert, G. Kothe, Transverse nuclear spin relaxation studies of viscoelastic properties of membrane vesicles: II. Experimental results, J. Phys. Chem., B 106 (2002) 5517–5526.
[30] D. Marsh, CRC Handbook of Lipid Bilayers, CRC Press, Boca Raton, FL, 1990.
[31] M. Bradl, Myelin dysfunction/degradation in the central nervous system: why are myelin sheaths susceptible to damage? J. Neural Transm., Suppl. 55 (1999) 9–17.
[32] E. Seboun, J.R. Oksenberg, A. Rombos, K. Usuku, D.E. Goodkin, R.R. Lincoln, M. Wong, D. Pham-Dinh, O. Boesplug-Tanguy, R. Carsique, R. Fitoussi, C. Gartioux, C. Reyes, F. Ribierre, S. Faure, C. Fizames, G. Gyapay, J. Weissenbach, A. Dautigny, J.B. Rimmler, M.E. Garcia, M.A. Pericak-Vance, J.L. Haines, S.L. Hauser, Linkage analysis of candidate myelin genes in familial multiple sclerosis, Neurogenetics 2 (1999) 155–162.
[33] D.R. Beniac, D.D. Wood, N. Palaniyar, F.P. Ottensmeyer, M.A. Moscarello, G. Harauz, Marburg's variant of multiple sclerosis correlates with a less compact structure of myelin basic protein, Mol. Cell. Biol. Res. Commun. 1 (1999) 48–51.
[34] J. Sedzik, A.E. Blaurock, Myelin vesicles: what we know and what we do not know, J. Neurosci. Res. 41 (1995) 145–152.
[35] D. Boison, H. Bussow, D. D'Urso, H.W. Muller, W. Stoffel, Adhesive properties of proteolipid protein are responsible for the compaction of CNS myelin sheaths, J. Neurosci. 15 (1995) 5502–5513.
[36] M.B. Bornstein, C.S. Raine, Initial structural lesion in serum-induced demyelination in vitro, Lab. Invest. 35 (1976) 391–401.
[37] D.L. Casper, D.A. Kirschner, Myelin membrane structure at 10 Å resolution, Nat., New biol. 231 (1971) 46–52.
[38] C. Linington, M.G. Rumsby, Accessibility of galactosyl ceramides to probe reagents in central nervous system myelin, J. Neurochem. 35 (1980) 983–992.
[39] D.A. Kirschner, A.L. Ganser, Myelin labeled with mercuric chloride. Asymmetric localization of phosphatidylethanolamine plasmalogen, J. Mol. Biol. 157 (1982) 635–658.